A Compact Helicon Thruster for CubeSat Applications

IEPC-2015-244／ISTS-2015-b-244

Presented at Joint Conference of 30th International Symposium on Space Technology and Science,
34th International Electric Propulsion Conference and 6th Nano-satellite Symposium
Hyogo-Kobe, Japan
July 4–10, 2015

David Biggs* , Sam Avery† , Luke Raymond‡ , Wei Liang§
Nicolas Gascon¶ , Andrea Lucca Fabris‖ , Juan Rivas-Davila**, Mark Cappelli††
Stanford University, Stanford, California, 94305, USA

This paper presents a preliminary experimental characterization of a compact helicon thruster for CubeSat applications operating on argon and water propellants. The helicon is powered by a compact radiofrequency inverter at 46.5 MHz and 88.4 MHz, which can be pulsed to enable efficient helicon generation while maintaining CubeSat attainable power levels. Ion population and electron temperature is approximated using spectroscopy. Ion velocity distributions and beam currents are evaluated using a retarding potential analyzer and guarded faraday probe for both argon and water propellants.

Nomenclature

RF	= radio-frequency
ω_{ce}	= electron cyclotron frequency
ω_{ci}	= ion cyclotron frequency
ω_{lh}	= lower hybrid plasma frequency
RPA	= Retarding Potential Analyzer
ϵ	= electron energy
m^*	= reduced mass
k_b	= Boltzmann's constant
T_e	= electron temperature

I. Introduction

A. Background

Electrodeless propulsion is a promising step in the technological evolution of electric propulsion, as it is able to overcome critical issues such as erosion and degradation of electrodes and the plasma channel wall. Acceleration grid erosion is a lifetime-limiting process in ion thrusters as is cathode and wall erosion in Hall thrusters. The absence of an external neutralizer is another attractive advantage that is offered by electrodeless propulsion systems.

In the last decade several efforts have been dedicated to the development of an electrodeless plasma thruster based on a helicon source.[1] As a result of their capability to work at different power regimes,

*Graduate Student, Mechanical Engineering, david.biggs@stanford.edu.
†Graduate Student, Aeronautics and Astronautics, sbavery@stanford.edu.
‡Graduate Student, Electrical Engineering, lraymond@stanford.edu.
§Graduate Student, Electrical Engineering, liangw@stanford.edu.
¶Research Scientist, Mechanical Engineering, nicolas.gascon@stanford.edu.
‖Postdoctoral Research Fellow, Mechanical Engineering, lfandrea@stanford.edu.
**Assistant Professor, Electrical Engineering, jmrivas@stanford.edu.
††Professor, Mechanical Engineering, cap@stanford.edu.

helicon thrusters may be a candidate for different mission scenarios, including satellite attitude control, drag compensation in LEO orbit, station keeping, and orbit transfer.

A helicon thruster consists of a helicon Radio-Frequency (RF) plasma source, characterized by an efficient ionization of the operating gas and a power deposition in the form of electron heating, leading to the production of higher density plasmas in comparison with other types of discharge (e.g. inductive and capacitive) at the same power level.[2,3] Helicons are wave modes propagating in a cylindrical, axially magnetized plasma column. Their frequency lies in the frequency region $\omega_{ci} < \omega_{lh} < \omega < \omega_{ce}$ where ω_{ce} and ω_{ci} are the ion and electron cyclotron frequencies and ω_{lh} is the lower-hybrid frequency. The waves propagate along the plasma column and the mode energy is absorbed by electrons through both collisional processes and collisionless damping.[1,2]

The acceleration stage can be a divergent magnetic field (magnetic nozzle),[4] a double-layer[5,6] or a selective heating system coupled with a magnetic nozzle.[7] The purpose of the magnetic nozzle is to convert plasma internal energy into directed kinetic energy, generating thrust for propulsion. The thrust acts on the magnetic field which becomes the mean to transfer the force to the spacecraft as in a physical de Laval nozzle. However, unlike a conventional nozzle, the magnetic field fills all space and the field lines close themselves. The plasma does not necessarily separate from the magnetic field, following the field lines and returning to the thruster. As a consequence, non-detached plasma does not provide thrust, therefore detachment is a fundamental phenomenon for propulsive purposes.[8]

Under certain conditions[9] a current-free electric double layer can build up in a helicon plasma expanding in a magnetic field. The double-layer is a plasma structure characterized by a steep potential drop which can provide an ion acceleration up to supersonic velocities.[5] This phenomenon can be exploited for propulsion applications as proposed by Charles[6] at the Australian National University.

The physical lay-out of a helicon thruster is simple and made of few elements: a feeding system to provide the incoming neutral gas flow; a dielectric tube where the plasma is generated; a helicon RF antenna wrapped around the glass tube; and an externally applied magnetic field generated by either a system of coils or permanent magnets.

The antenna is powered through an RF power network. The static magnetic field allows the propagation of electromagnetic waves in the plasma according to proper modes, increasing the plasma source efficiency in terms of power deposition. Moreover, it enhances plasma confinement and shapes the magnetic nozzle. The helicon plasma thruster presents potential advantages in comparison with the other electrical propulsion systems: the plasma marginally interacts with the structure therefore the erosion is reduced, internal and external electrodes are absent, the exhaust beam is neutral thus an external neutralizer is not needed, it is light and compact, and it can potentially work with different propellants.

Research projects in Australia,[6] USA,[7,10,11] Europe[12] and Japan[13,14] have been dedicated to this new technology, focusing both on fundamental physics[15] and on engineering aspects.[16] Different operating regimes have been explored in terms of power and mass flow rate.

The researchers of the Australia National University can be considered the pioneers of the helicon plasma thruster since they have been the first to propose the application of a helicon source to space propulsion. They have carried out several studies with different propellants (argon[17] and xenon[3]) in the power range 0.4 - 2 kW, both with electromagnets[3,17] and permanent magnets.[18] In a performance characterization,[18] they have obtained a thrust of 15 mN, specific impulse of 2000 s and a thrust efficiency of 8% for 2 kW of input power and a mass flow rate of 24 sccm of argon.

Helicon propulsion technology has been explored also in the high power range, particularly a helicon thruster operating in the range 20 - 100 kW has been developed and tested at University of Washington[11] (USA), achieving a thrust level of 1N and 2000 s of specific impulse for argon. Other tests with hydrogen have shown a specific impulse up to 8000 s.

A mini-helicon thruster has been studied at Massachusetts Institute of Technology[10] (USA) using nitrogen N_2 and argon as the propellants (flow rates within the range 10 - 50 sccm) and working in the power range 0.5 - 1 kW. The-mini helicon is characterized by a high-power-density and compactness in comparison with the system developed at ANU. The propulsive performances are: thrust 10 mN, specific impulse 1000-2000 s for Ar and 2000-4000 s for N_2 with thrust efficiencies up to 20%.

Extensive work on a low-power (50W - 1mN class) helicon thruster was carried out at the University of Padova (Italy). Several engineering aspects were explored and innovative elements were tested, including different magnetic field shapes, a ceramic diaphragm with reduced diameter at the thruster outlet, different working frequencies, and a plume screen.[12,16,19] A final prototype was designed and built in collaboration

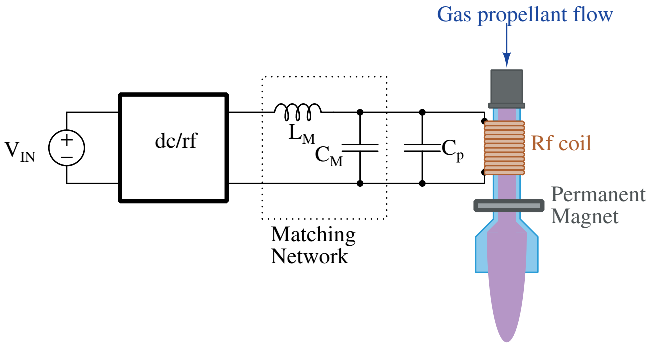

Figure 1. Power Processing and Delivery.

with the Kharkiv Aviation Institute (Ukraine), obtaining 0.5 mN at 0.12 mg/s of argon (420s I_{sp}) and an efficiency of 13%.[20] Numerical tools were also developed for designing helicon thrusters and exploring the use of alternative propellants.[21,22]

Finally helicon sources can be exploited as the primary source to produce a high-density ion flow in multi-stage thrusters as in the VASIMR (Variable Specific Impulse Magneto-plasma Rocket) project.[7]

B. Helicon Thruster and Radio Frequency Inverter

This paper presents an experimental characterization of a compact helicon thruster for CubeSat applications operating on argon and water propellants. The helicon is ignited in a 1.25 cm quartz tube using a novel axial antenna and is powered by a compact radiofrequency inverter capable of supplying up to 35 W at 40-90 MHz. A magnetic field designed for a strong cusp, ideal for a magnetic nozzle, is created using samarium cobalt magnets. The maximum magnetic field strength at the cusp was determined to be 2.5 kG.

The preliminary thruster design includes the 1.25 cm quartz tube, RF generation system, and magnet arranged in under 1/4 of a 1U (10x10x10 cm) aluminum cube skeleton. Liquid water propellant may be stored in the form factor of the CubeSat as needed to acheive given mission objectives. On the inside of the end plate, a samarium cobalt magnet is permanently attached to the wall to form a magnetic nozzle at the exit plane. A novel antenna encircles the thruster tube and connects to an RF inverter mounted to the end plate.

The helicon plasma system consists of an RF power amplifier, a matching network, and a plasma antenna as shown in Fig. 1. The helicon plasma is powered by a solid state switch mode RF power amplifier operating at a base switching frequency of tens of MHz.[23] The powersupply has the ability to be pulsed (modulated on and off) at lower frequency (mHz to MHz) between 0 and 100% duty cycle. Pulsed operation provides an efficient method of power modulation as well as an ability to maximize plasma energy and propellant utilization.

Resonant circuit operation allows for high efficiency operation at tens of MHz. The high base switching frequency allows for the exclusive use of air-core inductors and ceramic capacitors conducive to space operation. Further, passive component values are small enough at the frequencies used to allow them to be 3D printed or embedded in the printed circuit board.

Prototype amplifiers have been successfully tested on plasma loads with an average power of between 0.5 W and 35 W at electrical efficiencies above 90 percent. The current power supply implementation has a peak power density exceeding 50 W/in^3 allowing for multiple independent thruster units to be incorporated in a volume of less than 1U. Further, the current power supply can operate on a range of input voltages between 9 V and 50 V.

By controlling pulse frequency and pulse length one can determine whether the plasma discharge is primarily capacitive, primarily inductive, or some combination of the two. Fig. 2 shows voltage and current waveforms at the input of the matching network for a plasma discharge pulse that includes both modes. The discharge starts in capacitive mode and then transitions to inductive mode. The matching network was tuned such that the load impedance scene by the amplifier is resistive during inductive mode operation to optimize efficiency under higher power operation. Fig. 2 shows that voltage (green) and current (purple) waveforms are in phase during inductive operation.

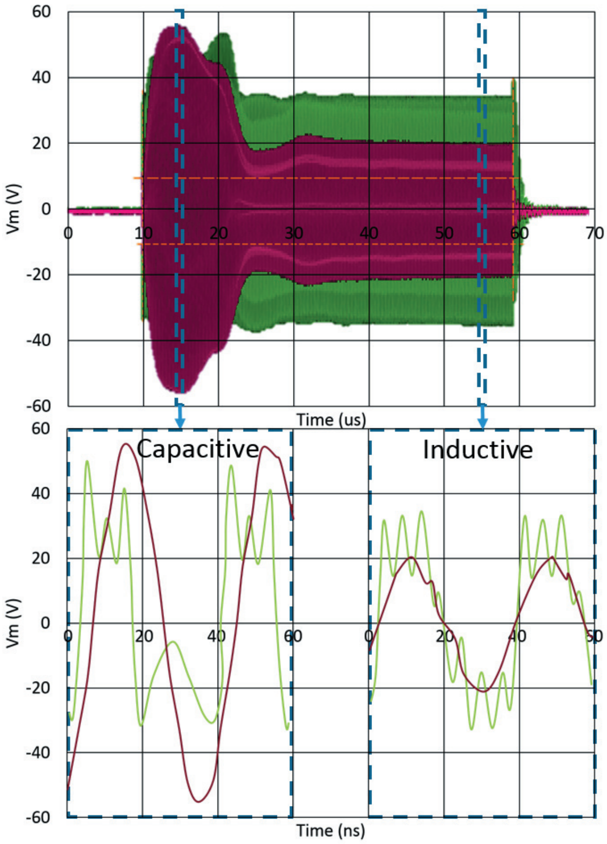

Figure 2. 50 us pulse with Capacitive-Inductive Transition.

II. Experimental Setup

Experiments were conducted in the Stanford Plasma Physics Laboratory small vacuum facility, with a custom quartz funnel (1.25 cm diameter to 5 cm diameter) attached to a vacuum chamber. A schematic of the experimental setup is shown in Fig. 3.

While developing the pulsed RF inverter, a preliminary experimental campaign was undertaken to characterize the plasma discharge in similar conditions. A continuous helicon discharge was sustained using a signal generator (HP 83732B) and RF power amplifier (ENI 320L) at 40 to 80 MHz. A novel antenna was self-resonated to produce a resistive load for the amplifier, but the matching network was not optimized to achieve full power transfer. For all test cases we expect less than 5 W transmitted power to the antenna.

Plasma diagnostic measurements were made using a retarding potential analyzer and Faraday probe. Both probes were attached to a linear translating stage within the vacuum chamber, placed 17.5 cm away from the thruster nozzle, in order to capture ion beam data at various radial positions, as shown in Fig. 4. A COSMOS stepper motor controller enabled probe positioning to an accuracy of 1.5×10^{-4} cm/step.

A. Retarding Potential Analyzer

The RPA is a standard plasma diagnostic tool used characterize the energy distribution of an ion beam. The probe acts as a energy filter by applying a variable positive potential across an internal grid to only allow high energy ions to be collected.[20] The RPA used was developed and discussed in previous work,[24] and is composed of four grids consisting of a (in order) floating, negatively biased electron repelling, positively biased ion retarding, and secondary electron suppression, all before a copper collection plate. The electron repelling grid was maintained at -40 V for nominal test cases while the ion retarding grid was swept from 0-250V.

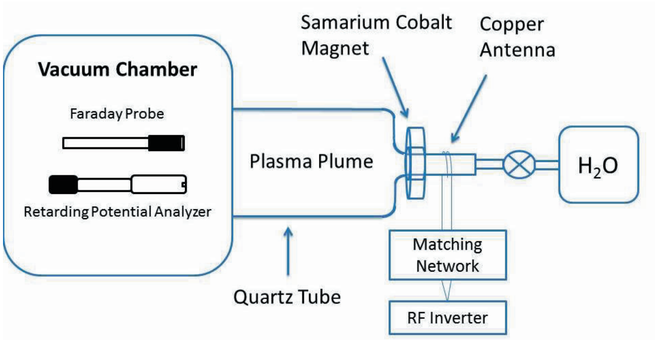

Figure 3. Experimental setup for helicon thruster testing.

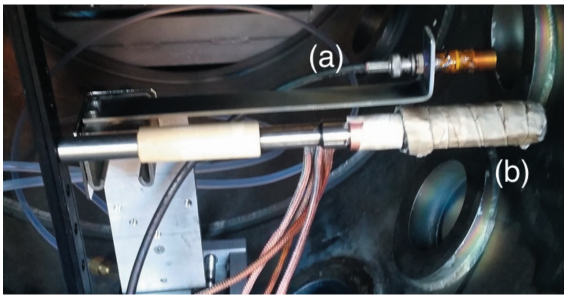

Figure 4. Faraday probe (a) and RPA (b) arrangement on a linear stage.

The secondary electron suppression grid remained floating as secondary electron emission was minimized by coating the collector plate with a conductive graphite paste. The final collector plate provided the ion beam current as a digital readout on a picoammeter (Keithley 485).

B. Faraday Probe

Total ion current was measured using a guarded Faraday probe with a 0.012m collector plate and a surrounding guard ring. Both the collector plate and the guard ring were biased to -40V to repel electrons and collect ion beam current at varying points along the plume. The Faraday probe was swept from -5 cm to +5 cm away from the center of the ion beam to obtain current versus position.

C. Vacuum Chamber

All ion velocity and total ion current measurements were obtained in a small vacuum chamber using cryogenic pumping. Pressure measurements were obtained using a hot-filament ionization gauge to detect pressures on the order of 10^{-6} - 10^{-5} Torr. This test facility consists of a non-magnetic stainless steel chamber approximately 0.6 m in diameter and 1.2 m in length. The chamber is pumped by a single 50 cm diameter cryopump (CVI-TM500) and initial rough vacuum pumping by a $\sim$60 L/s mechanical pump.

III. Results

The helicon thruster has been tested on both argon and water propellants, producing varying levels of thruster performance. Visually the plumes look very different, shown in Fig. 5. The argon plume is visibly blue, characteristic of excited argon ions,[19] and strongly follows the magnetic field of the magnet. There is a noticeable plasma beam in the center of the plume. The water plume is a more complicated structure with a central plasma beam surrounded by a dense plume and a diffuse plasma plume. The inner beam and dense plume follow the magnetic field lines, but the diffuse plume does not.

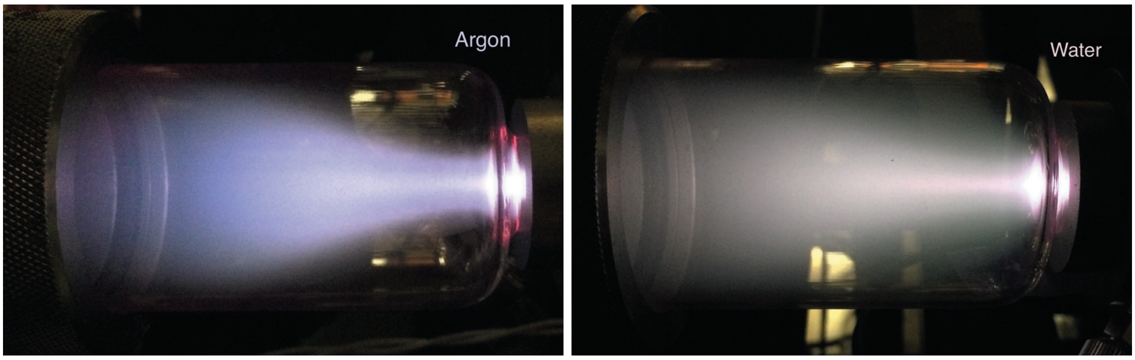

Figure 5. Photographs of plumes of argon (left) and water (right).

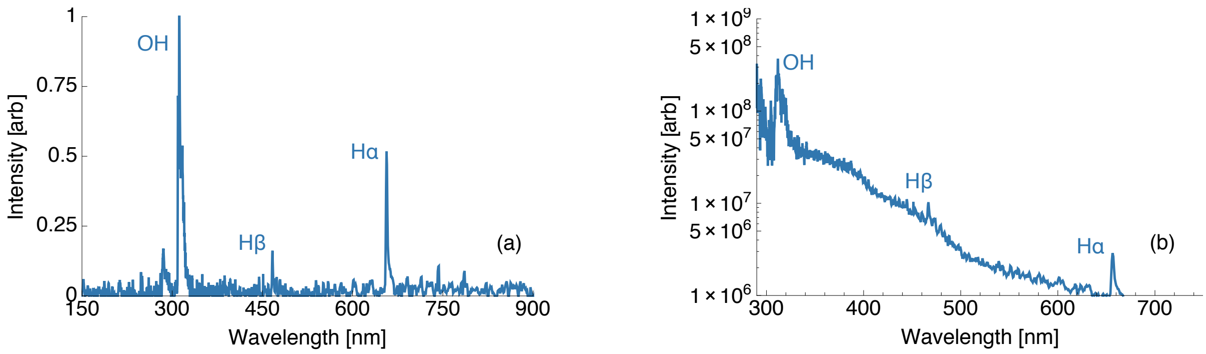

Figure 6. Intensity spectrum from emission of helicon with water propellant, (a) intensity uncalibrated, (b) intensity calibrated with a tungsten lamp.

A. Spectroscopy Measurements

The spectroscopy of the water plume using an Ocean Optics S2000 spectrometer is shown in Fig. 6 with both the intensity calibrated and uncalibrated. The dominant emission lines are that of OH, Hα, and Hβ, which agree with work by Nguyen et al.[25] A large volume of work has been conducted studying the collision reactions of water molecules with energetic electrons, which was compiled by Itikawa and Mason.[26] Within these results are collision cross sections for the electron impact dissociation of water and the subsequent emission of radiation from excited products, OH^* or H^*, as functions of electron temperature. The ratio of the two reaction cross sections, shown in Fig. 7 (a), can then be used to determine the electron temperature. For the helicon thruster experiment presented, it is predicted that there is a sub-population of electrons with energies of approximately 19 eV. Furthermore, ionization reaction cross sections are given by Itikawa and can be used to determine volumetric reaction rates by assuming a Maxwellian distribution of electrons, with Eqn. 1.

$$k_f(T_e) = \int_0^\infty f(\epsilon)\sqrt{\frac{2\epsilon}{m^*}}\sigma(\epsilon)\,d\epsilon \tag{1}$$

$$f(\epsilon) = 8\pi\left(\frac{1}{2\pi k_b T_e}\right)^{3/2}\sqrt{\frac{\epsilon}{2}}\exp\left(\frac{-\epsilon}{k_b T_e}\right)$$

Here, ϵ is the electron energy, m^* is the reduced mass, k_b is Boltzmann's constant, and T_e is the electron temperature. Finally, assuming a subset of hot electrons with a density of 10^{11} cm^{-3} responsible for ionization of water molecules, and a transit time of water molecules passing through a 1 cm long antenna at a mass flow rate of 15μg/s, the ion density of H_2O^+, OH^+, and H^+ are shown in Fig. 7 (b) as functions of electron temperature. For the helicon thruster experiment presented, the densities were estimated to be 3×10^{12} cm^{-3} for H_2O^+, 7×10^{11} cm^{-3} for OH^+, and 4×10^{11} cm^{-3} for H^+.

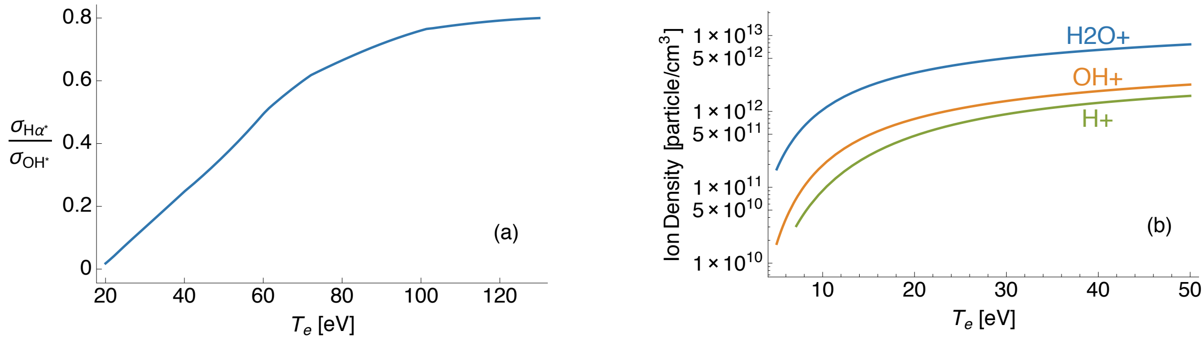

Figure 7. Ratio of collision cross sections for water and electron collisions producing H_α and OH emission lines.

B. Retarding Potential Analyzer Measurements

The ion energies were analyzed with the RPA for both argon and water propellants at 46.5 MHz, and an additional test for water at 88.4 MHz. It is assumed from our spectroscopic studies that for water the only ion species present are positively charged. It will require further work to investigate the effect of negative ions, if present. The data for the three test cases is shown in left column of Fig. 8. Each test case was performed at least twice on separate days to confirm repeatability. The argon RPA current-voltage is similar to that reported by Batishchev.[27] The RPA current-voltage from tests with water propellant show current drop-off and significantly higher voltages than that of argon. The integral of a Gaussian distribution, an error function shown in Fig. 2, was used to fit the data and determine the mean ion velocity, $\bar{v}$. For the helicon thruster presented, the mean ion velocities were approximated to be 26 km/s with argon at 46.5 MHz, 54 km/s with water at 46.5 MHz, and 65 km/s with water at 88.4 MHz.

$$\int n \exp\left[-\frac{(v-\bar{v})^2}{t}\right] dv = \frac{1}{2}\sqrt{\pi} n \sqrt{t}\,\mathrm{erf}\left(-\frac{v-\bar{v}}{\sqrt{t}}\right) + k \tag{2}$$

It is in general not a good assumption that the plasma in the plume of the thruster is thermalized to a Maxwellian distribution, and information about the nonthermal nature of the plasma is lost in this empirical fit. Nevertheless, this method provides an estimate of the mean ion velocity for performance characterization. The frequency dependence on ion velocity is plausibly due to greater forward power delivered to the plasma.

C. Faraday Probe Measurements

The total ion flux was measured by scanning the Faraday probe across the plume, data of which is shown in the right column of Fig. 8. The ion beam current was an order of magnitude higher for water than argon propellant, indicating greater ionization fraction from power coupling to the plasma.

Assuming angular symmetry, the Faraday probe data was integrated across the plume to find the total beam current, ranging from 0.05 - 0.35 mA. For argon propellant the ion mass flow rate is easily attained by assuming singly charged ions. For water the average mass of singly ionized particles based on the estimated species concentrations earlier was used. The thrust is then calculated to be on the order of 2 - 5 μN. The specific impulse is plotted for various propellant mass utilization fractions ($\dot{m}_i/\dot{m}_{total}$) in Fig. 9.

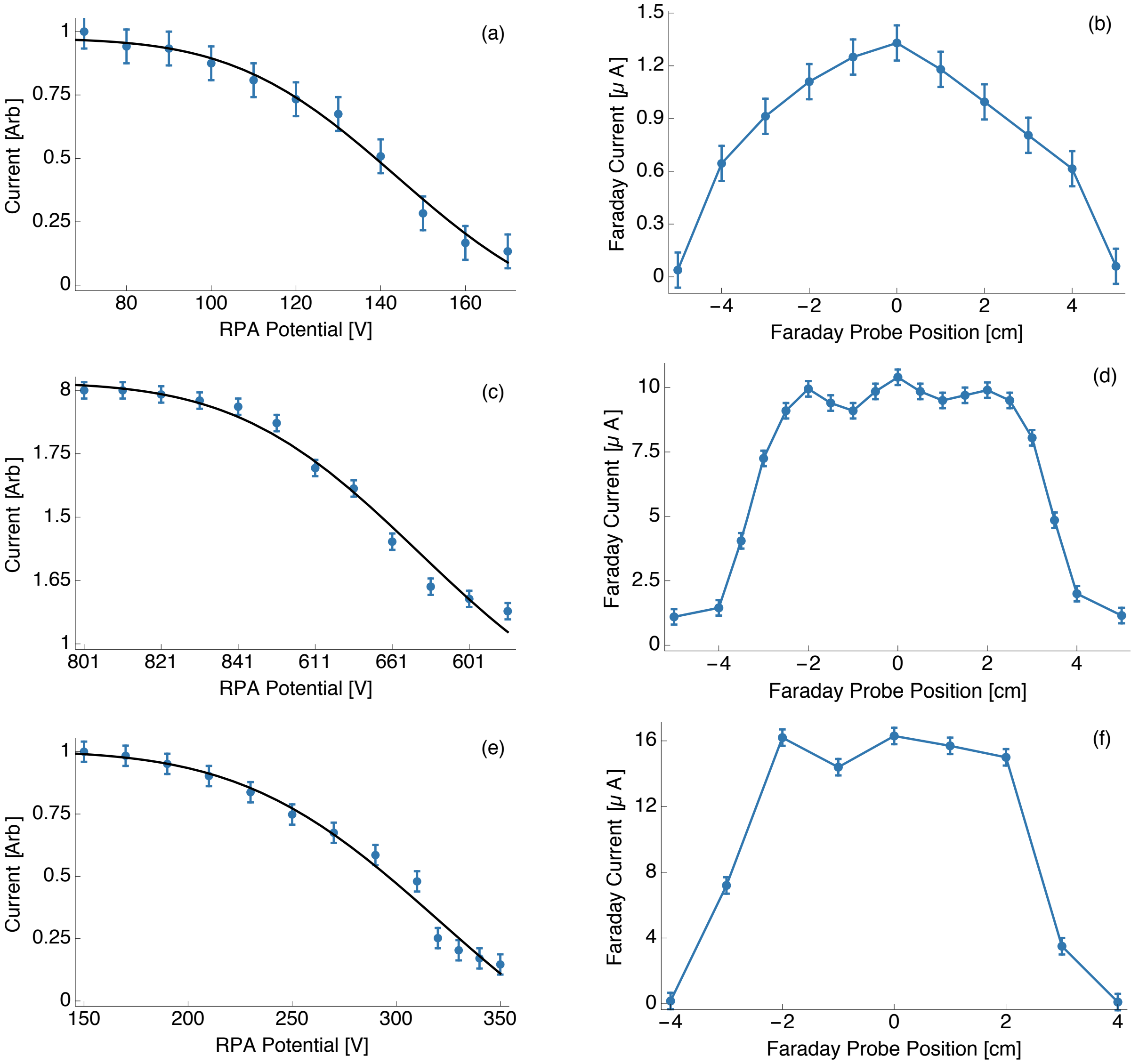

Figure 8. RPA and Faraday probe data for the helicon thruster with argon at 46.5 MHz (a,b), water at 46.5 MHz (c,d), and water at 88.4 MHz (e,f).

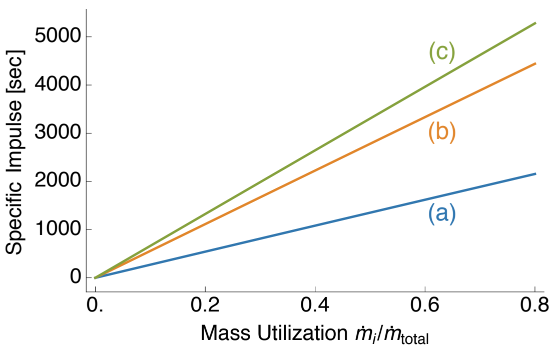

Figure 9. Approximate specific impulse for argon propellant at 46.5 MHz (a) and water propellant at 46.5 MHz (b) and 88.4 MHz (c) for a given propellant mass utilization fraction.

IV. Summary and Future Work

A compact helicon thruster for CubeSat applications has been tested with argon and water propellants. A compact RF inverter has been developed that can sustain the helicon discharge with either continuous or pulsed power. Preliminary RPA measurements identify argon ions with energies greater than 100 eV and water ions with energies greater than 200-300 eV. For water propellant, spectroscopy along with reactive collision cross section data is used to approximate the electron temperature of a sub-population to be 19 eV and ion species concentrations dominated by H_2O^+ at 10^{12} cm^{-3}. Faraday probe measurements show ion currents an order of magnitude higher for water than argon. Finally, performance metrics using RPA and Faraday probe data of the helicon thruster are reported achieving thrusts of 2 - 5 μN. Future work will include: 1) identify and limit mass flow rates to approach more optimal performance; 2) thrust stand measurements for both thrust and total impulse delivered for feasibility of missions; 3) RF compensated Langmuir probe measurements of plasma potential and electron temperature; 4) engineering design for propellant storage and delivery to push towards flight readiness.

References

[1] Chen, F. F. and Boswell, R. W., "Helicons-the past decade," *IEEE Transactions on Plasma Science*, Vol. 25, No. 6, 1997, pp. 1245–1257.

[2] Lieberman, M. and Boswell, R., "Modeling the transitions from capacitive to inductive to wave-sustained rf discharges," *Le Journal de Physique IV*, Vol. 8, No. PR7, 1998, pp. Pr7–145.

[3] West, M. D., Charles, C., and Boswell, R. W., "High density mode in xenon produced by a Helicon Double Layer Thruster," *Journal of Physics D: Applied Physics*, Vol. 42, No. 24, 2009, pp. 245201.

[4] Merino, M. and Ahedo, E., "Simulation of plasma flows in divergent magnetic nozzles," *IEEE Transactions on Plasma Science*, Vol. 39, No. 11, 2011, pp. 2938–2939.

[5] Charles, C. and Boswell, R., "Laboratory evidence of a supersonic ion beam generated by a current-free helicon double-layer," *Physics of Plasmas*, Vol. 11, 2004, pp. 1706.

[6] Charles, C., Boswell, R., Alexander, P., Costa, C., Sutherland, O., Pfitzner, L., Franzen, R., Kingwell, J., Parfitt, A., Frigot, P., et al., "Helicon double layer thrusters," *42nd. AIAA/ASME/SAE/ASEE Joint Propulsion Conference*, 2006.

[7] Bering, E., Longmier, B., Ballenger, M., Olsen, C., Squire, J., and Diaz, F., "Performance studies of the VASIMR® VX-200," *Proceedings of 49th AIAA Aerospace Sciences Meeting and Exhibit, Orlando, FL, USA*, 2011.

[8] Hooper, E., "Plasma detachment from a magnetic nozzle," *Journal of Propulsion and Power*, Vol. 9, No. 5, 1993, pp. 757–763.

[9] Ahedo, E., "Double-layer formation and propulsive assessment for a three-species plasma expanding in a magnetic nozzle," *Physics of Plasmas*, Vol. 18, 2011, pp. 033510.

[10] Batishchev, O. V., "Minihelicon plasma thruster," *IEEE Transactions on Plasma Science*, Vol. 37, No. 8, 2009, pp. 1563–1571.

[11] Ziemba, T., "High Power Helicon Thruster," *Proceedings of AIAA/ASME/SAE/ASEE 41st Joint Propulsion Conference, Tucson, AZ, USA*, July 2005.

[12] Pavarin, D., Ferri, F., Manente, M., Lucca Fabris, A., Trezzolani, F., Faenza, M., Tasinato, L., Tudisco, O., Deangelis, R., Loyan, A., Protsan, Y., Tsaglov, A., Selmo, A., Katsonis, K., Berenguer, C., Packan, D., Jarrige, J., Blanchard, C., Elias, P. Q., and Bonnet, J., "Thruster Development Set-up for the Helicon Plasma Hydrazine Combined Micro Research Project," *Proceedings of 32nd International Electric Propulsion Conference, Wiesbaden, Germany*, September 2011, IEPC-2011-241.

[13] Takahashi, K., Oguni, K., Yamada, H., and Fujiwara, T., "Ion acceleration in a solenoid-free plasma expanded by permanent magnets," *Physics of Plasmas*, Vol. 15, 2008, pp. 084501.

[14] Motomura, T., Shinohara, S., Tanikawa, T., Hada, T., Funaki, I., Nishida, H., Shamrai, K. P., Matsuoka, T., Otsuka, F., Rudenko, T. S., Ohno, E., Yokoi, K., and Nakamura, T., "Development of electrodeless electric propulsion systems using high-density helicon plasmas: The HEAT project," *Proceedings of General Assembly and Scientific Symposium*, 2011.

[15] Cox, W., Charles, C., Boswell, R., and Hawkins, R., "Spatial retarding field energy analyzer measurements downstream of a helicon double layer plasma," *Applied Physics Letters*, Vol. 93, No. 7, 2008, pp. 071505–071505.

[16] Pavarin, D., Ferri, F., Manente, M., Lucca Fabris, A., Trezzolani, F., Faenza, M., Tasinato, L., Curreli, D., Melazzi, D., Rondini, D., Tudisco, O., Deangelis, R., Loyan, A., Protsan, Y., Tsaglov, A., Selmo, A., Katsonis, K., Berenguer, C., Pessana, M., and Lancellotti, V., "Characterization of the Helicon Plasma Thruster of the EU FP7 HPH.com Program," *Space Propulsion Conference, Bordeaux, France*, May 2012.

[17] West, M. D., Charles, C., and Boswell, R. W., "Testing a helicon double layer thruster immersed in a space-simulation chamber," *Journal of Propulsion and Power*, Vol. 24, No. 1, 2008, pp. 134–141.

[18] Takahashi, K., Charles, C., and Boswell, R., "Performance characterization of a permanent-magnet helicon plasma thruster," *Bulletin of the American Physical Society*, Vol. 57, 2012.

[19] Pavarin, D., Lucca Fabris, A., Trezzolani, F., Manente, M., Faenza, M., Ferri, F., Selmo, A., Katsonis, K., and Berenguer, C., "Low Power RF Plasma Thruster Experimental Characterization," 2012.

[20] Trezzolani, F., Lucca Fabris, A., Pavarin, D., , Manente, M., Tsaglov, A., Loyan, A., and Rubalov, O., "Low Power Radio-Frequency Plasma Thruster Development and Testing," *Proceedings of 33rd International Electric Propulsion Conference, Washington, USA*, October 2013, IEPC-2013-153.

[21]Bosi, F., Lucca Fabris, A., Trezzolani, F., Manente, M., Melazzi, D., and Pavarin, D., "Modelling and Optimization of Electrode-less Helicon Plasma Thruster with Different Propellants," *50th AIAA/ASME/SAE/ASEE Joint Propulsion Conference*, 2014, pp. 28–30.

[22]Trezzolani, F., Selmo, A., Bosi, F., Melazzi, D., Lucca Fabris, A., Lancellotti, V., Manente, M., , and Pavarin, D., "Integrated Design Tools for RF Antennas for Helicon Plasma Thrusters," *50th AIAA/ASME/SAE/ASEE Joint Propulsion Conference*, 2014.

[23]Rivas, J. M., Han, Y., Leitermann, O., Sagneri, A. D., and Perreault, D. J., "A High-Frequency Resonant Inverter Topology With Low-Voltage Stress," Vol. 23, No. 4, 2008, pp. 1759–1771.

[24]Ito, T., Gascon, N., Crawford, W. S., and Cappelli, M. A., "Ultra-Low Power Stationary Plasma Thruster," *International Electric Propulsion Conference Paper*, Vol. 198, 2005, p. 2005.

[25]Nguyen, S. V., Foster, J. E., and Gallimore, A. D., "Operating a radio-frequency plasma source on water vapor," *Review of Scientific Instruments*, Vol. 80, No. 8, 2009, pp. 083503.

[26]Itikawa, Y. and Mason, N., "Cross sections for electron collisions with water molecules," *Journal of Physical and Chemical reference data*, Vol. 34, No. 1, 2005, pp. 1–22.

[27]Batishchev, O. V., "Minihelicon plasma thruster," *Plasma Science, IEEE Transactions on*, Vol. 37, No. 8, 2009, pp. 1563–1571.